Biophysical Chemistry 251 (2019) 106189

Contents lists available at ScienceDirect

Biophysical Chemistry

journal homepage: www.elsevier.com/locate/biophyschem

Nearest-neighbour parameters optimized for melting temperature prediction of DNA/RNA hybrids at high and low salt concentrations

Vivianne Basílio Barbosa[a], Erik de Oliveira Martins[b], Gerald Weber[a,*]

[a] Departamento de Fsica, Universidade Federal de Minas Gerais, 31270-901 Belo Horizonte, MG, Brazil
[b] Escola Politécnica, Centro Universitário do Leste de Minas Gerais, 35170-056 Coronel Fabriciano, MG, Brazil

HIGHLIGHTS

- Optimized nearest-neighbour DNA/RNA parameters were obtained.
- New low-salt parameters for DNA/RNA
- Curve-fitting melting temperatures resulted in better parameters.
- Using RNA/RNA salt correction, when necessary, is advised.
- Taking the average of DNA and RNA overestimates DNA/RNA stability

GRAPHICAL ABSTRACT

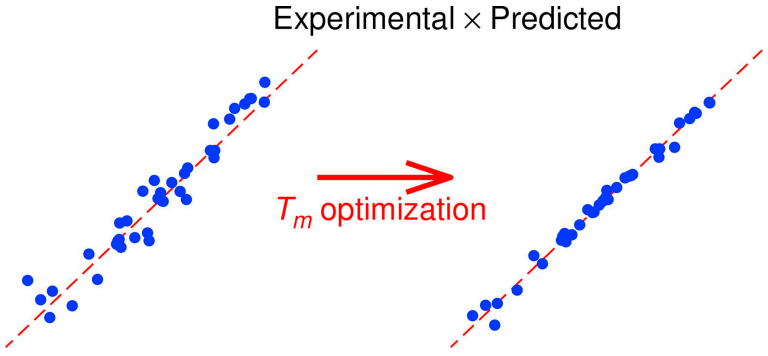

ARTICLE INFO

Keywords:
DNA
DNA/RNA hybrid
RNA stability
low sodium nearest-neighbour parameters

ABSTRACT

Gene editing technologies sparked a renewed interest in the hybridization of DNA/RNA duplexes, yet little improvement on nearest-neighbour parameters was made over the past two decades. For low sodium concentration no parameter set was yet calculated. Here, we revised the existing experimental datasets and used an expanded set of sequences from which we recalculated the nearest-neighbour parameters, reducing the average temperature prediction uncertainty to 1.6 °C. Two experimental sets using temperatures extracted via different methods were used with similar results, with the curve-fitting method achieving a slight advantage in prediction quality over other methods. Additionally, we obtained new parameters for low salt with an average uncertainty of 0.98 °C. We also tested several types of salt correction factors and concluded that it is advisable to use those originally developed for RNA/RNA rather than for DNA/DNA.

1. Introduction

Hybridization of short DNA-RNA (DR) sequences occurs during RNA polymerase [1] and is also central to the gene editing CRISPR-Cas9 technology [2]. The DR hybridization can be accurately modelled by statistical physics approaches [3], but linear models such as the nearest-neighbour (NN) model remain the method of choice for many applications due to its simplicity and for providing good predictions of melting temperatures. Currently, the NN parameters available for DR hybrids are from the pioneering work by Sugimoto et al. [4,5] and still to date they are the only parameters available for determining the secondary structures of DR hybrids [6,7]. For low salt concentrations we are not aware of any NN parameter set, even though melting temperature have been available for a long time [8].

* Corresponding author.
E-mail address: gweber@ufmg.br (G. Weber).

https://doi.org/10.1016/j.bpc.2019.106189
Received 24 April 2019; Received in revised form 14 May 2019; Accepted 14 May 2019
Available online 16 May 2019

The NN model typically relies on parameters calculated from total entropy and enthalpy variations. However, recently we showed that it can be advantageous to obtain them directly from the sequence melting temperatures [9,10]. The melting temperature optimization (MTO) method reduces the prediction uncertainty as it relies on measured temperatures and not on fitted sequence entropies and enthalpies. For the MTO method we developed the freely available software tool VarGibbs which can handle DNA-DNA (DD) and RNA-RNA (RR) duplexes, but was not originally designed for DR hybrids [9].

Here, we revisit the high salt NN parameters for DR hybrids using an expanded dataset of melting temperatures and derive new sets of parameters using the MTO method with a version of VarGibbs adapted for DR hybrids [9]. We prepared two separate datasets, one for melting temperatures obtained from the so-called curve fitting method (FT) and another composed of temperatures from the Van't Hoff ${T_m}^{-1} \times \log C_t$ plots (VH). The resulting parameters, for both FT and VH, were then compared against each other to evaluate the accuracy of the melting temperature predictions. Using a similar approach, we obtained the missing NN parameters for low salt concentrations from the melting temperatures, mostly from the work by Lesnik and Freier [8]. The accuracy of these new parameters are then compared to predictions using the NN parameters by Sugimoto et al. [5], after applying known salt corrections from DNA [11] and RNA [12].

2. Materials and methods

2.1. Melting temperature calculation

$\Delta {H_n}^{\mathrm{tot}}$ and $\Delta {S_n}^{\mathrm{tot}}$ are the total entropy and enthalpy variations of the nth sequence which may be obtained experimentally or can be calculated from nearest-neighbour schemes,

$$\Delta H_n^{tot} = \sum_i N_{ni} \Delta H_i, \quad \Delta S_n^{tot} = \sum_i N_{ni} \Delta S_i \tag{1}$$

where N_{ni} is the number of occurrences of elements of type i in the sequence. These elements can be nearest-neighbours or other sequence properties such as specific types of terminals, initiation factors or symmetry factors.

The melting temperature T_n for the nth sequence is calculated from [13].

$$T_n = \frac{\Delta H_n^{\mathrm{tot}}}{\Delta S_n^{\mathrm{tot}} + R \ln \frac{C_t}{f C_0}} \tag{2}$$

where $f = 4$ as all sequences are naturally non-self-complementary. R is the ideal gas constant, C_t is the species concentration, and $C_0 = 1\ \mu$M is the reference concentration.

The melting temperature optimization (MTO) method aims at minimizing the total difference between experimental T_i and predicted $T_i^{'}$ temperatures,

$$\chi^2 = \sum_{n=1}^{N} [T_n - T_n']^2 \tag{3}$$

where N the number of sequences. We also use the average absolute temperature difference

$$\langle | \Delta T | \rangle = \frac{1}{N} \sum_{n=1}^{N} |T_n - T_n'| \tag{4}$$

We also use this to compare the differences between melting temperature datasets, in this case T_i would be from one set and $T_i^{'}$ from the other.

2.2. Notation and melting temperature dataset

For the hybrid DR duplex we follow the usual notation dA, dC, dG and dT for the DNA bases and rU, rG, rC and rA for RNA, such that the base pairs are described as dArU, dCrG, dGrC and dTrA. Nearest neighbour base-pairs are represented as in the following example

$$\begin{matrix} {}^{5'}\mathrm{r(UA)}^{3'} \\ {}^{3'}\mathrm{d(AT)}^{5'} \end{matrix} \leftrightarrow \begin{matrix} {}^{5'}\mathrm{d(TA)}^{3'} \\ {}^{3'}\mathrm{r(AU)}^{5'} \end{matrix} \rightarrow \mathrm{dTrA - dArU} \tag{5}$$

Note that dTrA–dArU is same as rUdA–rAdT, therefore for simplicity, in this work will always use the notation starting with the deoxy base.

We collected 70 DR sequences from Sugimoto et al. [5,14], 41 sequences from Wu et al. [15] and 4 sequence from Rauzan et al. [16], all at 1 M [Na^+]. One should note that most sequences from Ref. [15], are repeated from those of Ref. [5], so that the number of unique sequences is much lower. For each sequence we collected two temperatures, one measured with the curve-fitting method (FT, Supplementary Table S1) and the other one by the Van't Hoff adjustment (VH, Supplementary Table S2). We will refer to these datasets as D-DRFT (curve-fitting) and D-DRVH (Van't Hoff), which contain the same DR sequences but different melting temperatures. If we apply Eqs. (3) and (4), using D-DRFT as T_n and D-DRVH as $T_n^{'}$, we arrive at an average difference of $\langle | \Delta T | \rangle = 1.13\ ^{\circ}$C and $\chi^2 = 253\ (^{\circ}\mathrm{C})^2$. For low salt, 100 mM [$Na^+$], we collected 38 sequences from several sources [8, 17–20] of which the largest (28 sequences) were from Lesnik and Freier [8]. We refer to the low-salt dataset as D-DRLS (Supplementary Table S3), and unlike for the other high-salt datasets it was not possible to divide them into different measurement techniques.

2.3. Minimization procedure

For the multi-dimensional minimization of Eq. (3) we use the downhill simplex method [21]. The main numerical problem is the occurrence of local minima which makes it difficult to find the global best value of χ^2. For a given set of initial parameter values there is the inherent risk that the lowest value of χ^2 returned by the algorithm may be a local minima. To mitigate this problem we repeat the minimization for a large number of different initial parameters. The strategy for selecting the initial values is to use what we call seed parameters. Each time, we perform a complete minimization by randomly selecting new initial parameters within a certain vicinity of the seed parameters.

2.3.1. First minimization round

Here we used as seed parameters −8.0 kcal/mol and −30.0 cal/mol·K, for the enthalpy and entropy variation, respectively. The initial values were selected randomly within ± 50% of these seed values. Minimizations were carried out separately for D-DRFT, D-DRVH and D-DRLS datasets. We performed 1000 different minimization rounds, each time starting with different initial parameters. The final results were averaged over the minimized parameters of all rounds.

2.3.2. Second minimization round

We use the results of the first minimization round as new initial parameters. This time, we always start from the same initial parameters and vary the experimental data by small amounts using a Gaussian distribution such that the standard deviation of the original and perturbed data amounts to 0.5 °C. The resulting parameters are the average parameters over 1000 minimizations and the associated uncertainties are taken from the standard deviation. The final parameter sets are identified by the notation AOP (averaged optimized parameters) and the original datasets they were derived from. For instance, AOP-DRFT are the averaged optimized parameters obtained from dataset D-DRFT.

2.4. Availability

All parameters, datasets and software used in this work, are freely available from https://download.opensuse.org/repositories/home:/

Table 1
NN model parameters used in this study. P-SG95 are the original parameters from Ref. [5], FT (AOP-DRFT) and VH (AOP-DRVH) are the average optimized parameters for 1000 mM [Na^+] and LS (AOP-DRLS) are the optimized parameters for 100 mM [Na^+].

NN	ΔH_{NN} (kcal/mol)				ΔS_{NN} (cal/mol·K)			
	P-SG95	FT	VH	LS	P-SG95	FT	VH	LS
dArU-dArU	−11.5	−8.27	−7.72	−10.9	−36.4	−25.2	−23.9	−35.9
dArU-dCrG	−7.80	−9.39	−11.5	−10.2	−21.6	−25.2	−31.7	−29.0
dArU-dGrC	−7.00	−10.9	−10.6	−8.60	−19.7	−31.0	−30.0	−23.0
dArU-dTrA	−8.30	−9.90	−9.86	−9.47	−23.9	−28.6	−28.5	−30.5
dCrG-dArU	−10.4	−9.79	−10.7	−9.55	−28.4	−26.3	−29.0	−25.2
dCrG-dCrG	−12.8	−11.9	−11.4	−11.8	−31.9	−28.2	−26.5	−30.8
dCrG-dGrC	−16.3	−12.6	−13.0	−11.9	−47.1	−33.7	−35.2	−29.9
dCrG-dTrA	−9.10	−12.3	−12.2	−12.2	−23.5	−33.1	−33.0	−33.2
dGrC-dArU	−8.60	−11.5	−11.7	−8.70	−22.9	−33.0	−33.0	−25.6
dGrC-dCrG	−8.00	−13.5	−14.1	−8.42	−17.1	−34.5	−35.7	−22.4
dGrC-dGrC	−9.30	−12.4	−12.4	−7.47	−23.2	−32.9	−32.9	−19.3
dGrC-dTrA	−5.90	−11.7	−10.6	−12.7	−12.3	−31.0	−27.3	−37.9
dTrA-dArU	−7.80	−9.56	−10.2	−9.93	−23.2	−28.9	−30.9	−30.8
dTrA-dCrG	−5.50	−9.77	−9.60	−12.2	−13.5	−25.5	−24.4	−33.9
dTrA-dGrC	−9.00	−11.5	−10.7	−13.9	−26.1	−32.1	−29.9	−38.0
dTrA-dTrA	−7.80	−10.3	−9.93	−10.7	−21.9	−29.9	−28.6	−32.0
Initiation	1.90	1.49	1.59	0.963	−3.90	−8.51	−8.65	−6.51

Table 2
Quality parameters $\langle\Delta T\rangle$ and χ^2 for P-SG95 [4,5] and optimized AOP-DRFT/VH parameters applied on D-DRFT/VH sequences.

Parameters	Applied on	[Na^+] mM	Validation type	$\langle\Delta T\rangle$ (°C)	χ^2 (°C^2)
P-SG95	D-DRFT	1000	–	2.34	1109
P-SG95	D-DRVH	1000	–	2.28	1020
AOP-DRFT	D-DRFT	1000	self-validation	1.57	486.0
AOP-DRVH	D-DRVH	1000	self-validation	1.57	444.5
AOP-DRFT	D-DRVH	1000	cross-validation	1.66	491.1
AOP-DRVH	D-DRFT	1000	cross-validation	1.61	524.8

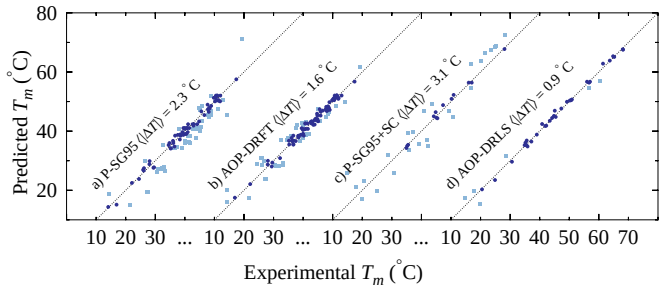

Fig. 1. Correlation of predicted and experimental melting temperatures for DR hybrids. The closer the data points are to the dotted diagonal lines the better the prediction accuracy. Blue bullets are predictions closer than 2.0 °C to the experimental data points, otherwise they are shown as light blue boxes. Panel (a) shows the prediction for the original parameters P-SG95 by Sugimoto et al. [5] when applied to dataset D-DRFT; (b) the optimized parameters AOP-DRFT when applied to dataset D-DRFT; (c) the prediction for the P-SG95 parameters after applying the RNA salt correction [12] for dataset D-DRLS; and (d) the optimized parameters AOP-DRLS for dataset D-DRLS. (For interpretation of the references to colour in this figure legend, the reader is referred to the web version of this article.)

drgweber/. A web interface is available at https://bioinf.fisica.ufmg.br/app/comparetm.pl where the parameters can be selected with the same notation as used here.

3. Results and discussion

One purpose of this work, apart from obtaining optimized parameters, was to investigate the differences of applying the MTO method on melting temperature datasets that were obtained using different

Table 3
Quality parameters $\langle\Delta T\rangle$ and χ^2 for parameters applied to low-salt D-DRLS sequences. For high-salt parameters P-SG95 [4,5], AOP-DRFT, and AOP-DRVH the calculated melting temperatures were corrected afterwards to 100 mM with DD corrections from Owczarzy et al. [11] and RR from Chen and Znosko [12].

Parameters	Salt correction	Validation type	$\langle\Delta T\rangle$ (°C)	χ^2 (°C^2)
P-SG95	DD [11]	cross-validation	3.50	676.4
P-SG95	RR [12]	cross-validation	3.11	566.8
AOP-DRVH	DD [11]	cross-validation	2.92	485.1
AOP-DRVH	RR [12]	cross-validation	2.63	457.3
AOP-DRFT	DD [11]	cross-validation	2.86	500.8
AOP-DRFT	RR [12]	cross-validation	2.57	460.7
AOP-DRLS	no correction	self-validation	0.945	73.36

approaches that are commonly used, namely the curve fitting method (FT) and the Van't Hoff $T_m^{-1} \times \log C_t$ plots (VH). For this reason, the parameter optimization was performed independently on the two datasets D-DRFT and D-DRVH. The final averaged enthalpy and entropy parameters, AOP-DRFT and AOP-DRVH, are shown in Table 1. These high-salt concentration parameters, AOP-DRFT and AOP-DRVH, are generally very close to each other and we noticed no important differences that could potentially lead to different interpretations of their physical significance. However, there are important differences when compared to P-SG95 from Sugimoto et al. [4,5], see Table 1. For instance, the stability of dCrG-dGrC NNs are considerably reduced for both AOP-DRFT and AOP-DRVH. On the other hand, this reduced stability appears to be compensated by an increased stability for dGrC-dGrC and dGrC-dCrG. The P-SG95 were originally obtained from a smaller subset of melting temperature data and via a different method which optimises for enthalpy and entropy differences rather than optimising for temperature predictions as in this work. Much larger differences are observed for the low-salt AOP-DRLS parameters, see Table 1, which is not unexpected considering the generally large effects that we have previously observed for DD [9] and RR [10] under similar low-salt conditions. Unfortunately, we are not aware of other parameter sets for the low salt concentration to which we could compare our AOP-DRLS results.

The comparison of melting temperatures from the two high-salt dataset, D-DRFT and D-DRVH, result in an average absolute difference of $\langle|\Delta T|\rangle = 1.13$ °C and $\chi^2 = 253$ (°C)^2, which sets a lower limit from what could be expected in the MTO method. For the unoptimised parameters P-SG95 applied on D-DRFT we obtain a $\langle|\Delta T|\rangle$ of 2.34 °C and $\chi^2 = 1109$ (°C)^2 and the optimization process reduces the merit

Table 4
Additional melting temperature data for low-salt DR hybrids under various buffer conditions. T_i are the reported experimental temperatures; T_i' and T_i'' are the predicted temperatures calculated using parameters AOP-DRLS and P-SG95, respectively. Predicted temperatures that are closer to the experimental data are underlined. All temperatures are in °C, sodium concentrations [Na^+] in mM, and strand concentrations C_t in μM. RNA salt corrections [12] were applied whenever salt concentrations differed from 100 mM.

Main strand 5′-3′	T_i	T_i'	T_i''	[Na^+]	C_t	Conditions
d(CCTAAATTTGCC)	26.2	<u>26.7</u>	29.3	20	4	20 mM sodium phosphate buffer, pH 6.8 [25]
d(TTTTCTTTTCCCCCCT)	60.0	<u>59.0</u>	64.5	110	1.5	2.5 mM Na_2HPO_4, 5.0 mM NaH_2PO_4, 0.1 EDTA, pH 7.0 [26]
d(GCGTTTTTTGCT)	45.0	<u>45.8</u>	48.3	100	8	10 mM phosphate buffer, ph 7.2 [27]
d(GCGTTTTTTTTTTGCG)	39.7	38.2	<u>38.5</u>	20	1.5	10 mM phosphate buffer, pH 7.0 [28]
r(GCAUCAGCAU)	40.1	<u>40.9</u>	39.2	100	16	0.1 EDTA, pH 7.0, DSC measurements [29]

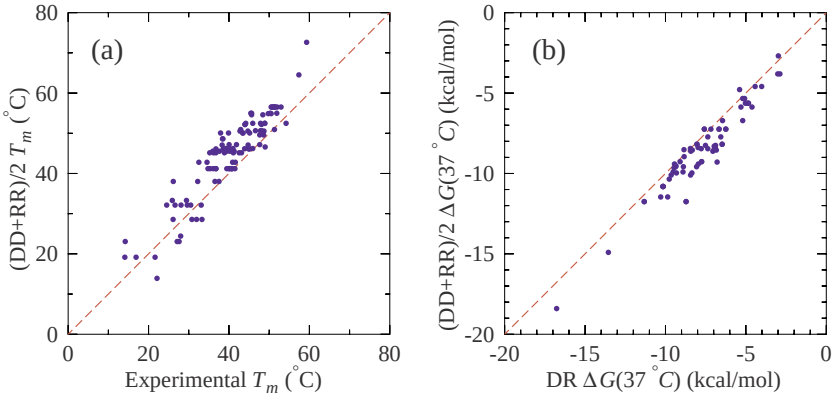

Fig. 2. Scatter plots of (a) melting temperatures calculated using averaged DD and RR parameters compared to experimental melting temperatures from dataset D-DRFT, and (b) Gibbs free energies calculated using averaged DD and RR parameters compared to energies calculated from parameters AOP-DRFT.

factor χ^2 to roughly half this value, as shown in Table 2. Here we use the same concept of self-validation as in [9], when the quality parameters $\langle\Delta T\rangle$ and χ^2 are applied to the same dataset from which these parameters were derived. An example of self-validation is when we apply the AOP-DRFT parameters to the D-DRFT melting temperature data, since D-DRFT was used to obtain the AOP-DRFT parameters. We use the term cross-validation when the parameters are applied to a different melting temperature dataset, as in the case of AOP-DRFT parameters applied to D-DRVH. As shown in Table 2, both cross-validation result in slightly larger merit factors than the corresponding self-validations. The prediction quality is also illustrated by the scatter plots shown in Fig. 1. For AOP-DRFT the prediction temperatures are generally clustered closer to the diagonal line, Fig. 1b, and showing fewer outliers than those for P-SG95, Fig. 1a. Overall, the prediction accuracy is better for sequences longer than 9 base pairs, see Supplementary Fig. S1, which are much closer to the diagonal line than for shorter sequences. For longer sequences the end effects and therefore terminal related initiation parameters, which were not explicitly taken into account, have less influence over the melting temperature prediction quality.

For the low-salt concentration melting temperatures, at 100 mM [Na^+], we first used the P-SG95 parameters and then applied either a DD [11] or RR [12] salt correction factors, the prediction quality is shown in Table 3. Similarly, we repeated this with the high-salt parameters AOP-DRFT and AOP-DRVH. Regarding the salt correction factors, both authors [11,12] propose a number of different schemes, here we use the ones that were considered to give the best results. Clearly, in all cases the RR salt correction factor [12] has better results, which corroborates numerous observations that DR hybrids tend to be more similar to RR duplexes, especially regarding the helix type which is considered closer to A-RNA [22–24]. The high-salt parameters AOP-DRFT and AOP-DRVH also outperform the older P-SG95 parameters in all cases, and here also the AOP-DRFT has better prediction quality than AOP-DRVH. This is consistent with our observations for high-salt sequences that AOP-DRFT is overall the best parameter set, as shown in Table 2, and can also be regarded as a validation of the high-salt parameters as they are unrelated to the D-DRLS dataset. The optimized low-salt parameters AOP-DRLS evidently perform much better than any combination of high-salt and salt correction factors, as shown in the last entry of Table 3. This is illustrated in Fig. 1, panels (c) and (d), where we show the scatter plots of the predicted and measured melting temperatures. In particular, for the optimized parameters the data points lie very close to the diagonal line. Here the self-prediction accuracy appears to be better that for the high-salt parameters, despite the fact that these temperatures come from various different sources [8,17–20]. However, we can not rule out that the better self-prediction could be due to the fact that the D-DRLS is a much smaller dataset, with only 38 temperatures. For smaller datasets it is generally easier to obtain parameters with better self-prediction capability as they only need to satisfy a reduced number of constraints, and the overly low $\langle|\Delta T|\rangle$ of AOP-DRLS in Table 3 is a clear indication of this.

Given the very low $\langle|\Delta T|\rangle$ of AOP-DRLS it would be desirable to test these parameters on an independent sequence set. Unfortunately, we were unable to find enough independent low-salt DR melting temperatures that could be used to form an independent validation dataset. The few independent low-salt DR sequences that we were able to identify were mostly single control sequences from various studies of modified DNA or RNA [25–29], under varying buffer conditions and are summarised in Table 4. The prediction accuracy appears to favour AOP-DRLS: in four out of five temperatures it resulted in better predictions than the P-SG95 parameters with RR salt corrections. Note that here also we had to salt-correct the AOP-DRLS in several cases. Therefore, while the optimistic quality parameters $\langle\Delta T\rangle$ and χ^2 of AOP-DRLS call out for some caution, the tests shown in Table 4 are encouraging nevertheless.

Apart from DR double helices, there is hardly any data that could be used to calculate NN parameters for more complicated secondary structures such as loops and bulges. This has lead some authors use the simple average of DD and RR parameters [6,7] to replace actual DR parameters for these structures. While we do not deal with loops and

bulges here, we can nevertheless verify the overall effect of taking the simple average of DD and RR parameters for the double helix to gain some insight regarding the stability bias that such approximation may induce. In Fig. 2a we show the melting temperature prediction using average of DD [9] and RR [10] parameters which shows that these parameters typically overestimate the DR stability. On average the deviation is $\langle|\Delta T|\rangle = 5.0$ °C and $\chi^2 = 3928$ °C^2. Similarly, the calculated Gibbs free energies shown in Fig. 2b are typically much lower for the average parameters equally indicating a higher duplex stability than using the optimized parameters. From this we conclude that the use of average DD and RR parameters generally overestimates the DR stability.

4. Conclusions

The new parameters for DNA/RNA hybrids have consistently better melting temperature prediction accuracy. Our tests indicate that this prediction quality is improved when the enthalpy and entropy parameters are derived form melting temperatures using the curve-fitting method. We also obtained low-salt parameters with good prediction quality which out perform any other high-salt parameters used in conjunction with salt-correction factors. Also, we noted that RNA/RNA salt-correction factors are generally better than DNA/DNA which is consistent with various observations of the RNA-like nature of DNA/RNA hybrids. Finally, we verified the idea of using averages of DNA/DNA and RNA/RNA parameters when the corresponding DNA/RNA are unavailable, as for instance in the case of bulges and loops. We found that in general these average parameters overestimate the stability of the hybrid duplex.

Acknowledgements

This work was supported by Fundação de Amparo a Pesquisa do Estado de Minas Gerais (Fapemig), Brazil; Conselho Nacional de Desenvolvimento Cientfico e Tecnolgico (CNPq), Brazil; and Coordenação de Aperfeiçoamento de Pessoal de Nível Superior (CAPES), Brazil.

Appendix A. Supplementary data

Supplementary Fig. S1 shows the sequence length dependency of the predictions, and tables S1–S3 show the sequences used for parameter optimizations. Supplementary data to this article can be found online at https://doi.org/10.1016/j.bpc.2019.106189.

References

[1] A. Aguilera, B. Gómez-González, DNA-RNA hybrids: the risks of DNA breakage during transcription, Nat. Struct. Mol. Biol. 24 (5) (2017) 439–443.
[2] M. Jinek, K. Chylinski, I. Fonfara, M. Hauer, J.A. Doudna, E. Charpentier, A programmable dual-RNA–guided DNA endonuclease in adaptive bacterial immunity, Science 337 (6096) (2012) 816–821.
[3] E.D.O. Martins, V.B. Barbosa, G. Weber, DNA/RNA hybrid mesoscopic model shows strong stability dependence with deoxypyrimidine content and stacking interactions similar to RNA/RNA, Chem. Phys. Lett. 715C (2019) 14–19, https://doi.org/10.1016/j.cplett.2018.11.015.
[4] N. Sugimoto, M. Katoh, S.-i. Nakano, T. Ohmichi, M. Sasaki, RNA/DNA hybrid duplexes with identical nearest-neighbor base-pairs have identical stability, FEBS Lett. 354 (1) (1994) 74–78.
[5] N. Sugimoto, S.-i. Nakano, M. Katoh, A. Matsumura, H. Nakamuta, T. Ohmichi, M. Yoneyama, M. Sasaki, Thermodynamic parameters to predict stability of RNA/DNA hybrid duplexes, Biochem 34 (35) (1995) 11211–11216.
[6] R. Lorenz, I.L. Hofacker, S.H. Bernhart, Folding RNA/DNA hybrid duplexes, Bioinformatics 28 (19) (2012) 2530–2531.
[7] F. Alkan, A. Wenzel, C. Anthon, J.H. Havgaard, J. Gorodkin, CRISPR-Cas9 off-targeting assessment with nucleic acid duplex energy parameters, Genome Biol. 19 (1) (2018) 177.
[8] E.A. Lesnik, S.M. Freier, Relative thermodynamic stability of DNA, RNA, and DNA:RNA hybrid duplexes: relationship with base composition and structure, Biochem 34 (34) (1995) 10807–10815.
[9] G. Weber, Optimization method for obtaining nearest-neighbour DNA entropies and enthalpies directly from melting temperatures, Bioinformatics 31 (6) (2015) 871–877, https://doi.org/10.1093/bioinformatics/btu751 http://bioinformatics.oxfordjournals.org/content/31/6/871.
[10] I. Ferreira, E.A. Jolley, B.M. Znosko, G. Weber, Replacing salt correction factors with optimized RNA nearest-neighbour enthalpy and entropy parameters, Chem. Phys. 521 (2019) 69–76, https://doi.org/10.1016/j.chemphys.2019.01.016 (URL doi: 10.1016).
[11] R. Owczarzy, Y. You, B.G. Moreira, J.A. Manthey, L. Huang, M.A. Behlke, J.A. Walder, Effects of sodium ions on DNA duplex oligomers: improved predictions of melting temperatures, Biochem 43 (2004) 3537–3554.
[12] Z. Chen, B.M. Znosko, Effect of sodium ions on RNA duplex stability, Biochem 52 (42) (2013) 7477–7485, https://doi.org/10.1021/bi4008275.
[13] S. Schreiber-Gosche, R.A. Edwards, Thermodynamics of oligonucleotide duplex melting, J. Chem. Educ. 86 (5) (2009) 644.
[14] N. Sugimoto, M. Nakano, S.-i. Nakano, Thermodynamics- structure relationship of single mismatches in RNA/DNA duplexes, Biochemistry 39 (37) (2000) 11270–11281.
[15] P. Wu, S. Nakano, N. Sugimoto, Temperature dependence of thermodynamic properties for DNA/DNA and RNA/DNA duplex formation, Eur. J. Biochem. 269 (12) (2002) 2821–2830 http://www.blackwell-synergy.com/doi/abs/10.1046/j.1432-1033.2002.02970.x.
[16] B. Rauzan, E. McMichael, R. Cave, L.R. Sevcik, K. Ostrosky, E. Whitman, R. Stegemann, A.L. Sinclair, M.J. Serra, A.A. Deckert, Kinetics and thermodynamics of DNA, RNA, and hybrid duplex formation, Biochem 52 (5) (2013) 765–772.
[17] J.I. Gyi, G.L. Conn, A.N. Lane, T. Brown, Comparison of the thermodynamic stabilities and solution conformations of DNA RNA hybrids containing purine-rich and pyrimidine-rich strands with DNA and RNA duplexes, Biochem 35 (38) (1996) 12538–12548.
[18] S. Wang, E.T. Kool, Origins of the large differences in stability of DNA and RNA helixes: C-5 methyl and 2′-hydroxyl effects, Biochem 34 (12) (1995) 4125–4132.
[19] A.M. Kawasaki, M.D. Casper, S.M. Freier, E.A. Lesnik, M.C. Zounes, L.L. Cummins, C. Gonzalez, P.D. Cook, Uniformly modified 2′-deoxy-2′-fluoro-phosphorothioate oligonucleotides as nuclease-resistant antisense compounds with high affinity and specificity for RNA targets, J. Med. Chem. 36 (7) (1993) 831–841.
[20] S. Nakano, M. Fujimoto, H. Hara, N. Sugimoto, Nucleic acid duplex stability: influence of base composition on cation effects, Nucleic Acids Res. 27 (14) (1999) 2957.
[21] W.H. Press, S.A. Teukolsky, W.T. Vetterling, B.P. Flannery, Numerical Recipes in C, Cambridge University Press, Cambridge, 1988.
[22] J.I. Gyi, A.N. Lane, G.L. Conn, T. Brown, Solution structures of DNA.RNA hybrids with purine-rich and pyrimidine-rich strands: comparison with the homologous DNA and RNA duplexes, Biochem 37 (1) (1998) 73–80.
[23] Y. Xiong, M. Sundaralingam, Crystal structure of a DNA.RNA hybrid duplex with a polypurine RNA r(gaagaagag) and a complementary polypyrimidine DNA d (CTCTTCTTC), Nucleic Acids Res. 28 (10) (2000) 2171–2176.
[24] M. Nowotny, S.A. Gaidamakov, R.J. Crouch, W. Yang, Crystal structures of RNase H bound to an RNA/DNA hybrid: substrate specificity and metal-dependent catalysis, Cell 121 (7) (2005) 1005–1016.
[25] A.P. Beevers, K.J. Fettes, G. Sabbagh, F.K. Murad, J.R. Arnold, R. Cosstick, J. Fisher, NMR and UV studies of 3-S-phosphorothiolate modified DNA in a DNA:RNA hybrid dodecamer duplex; implications for antisense drug design, Org. Biomol. Chem. 2 (1) (2004) 114–119.
[26] M. Hornum, P. Kumar, P. Podsiadly, P. Nielsen, Increasing the stability of DNA:RNA duplexes by introducing stacking phenyl-substituted pyrazole, furan, and triazole moieties in the major groove, J. Organ. Chem. 80 (19) (2015) 9592–9602.
[27] M.A. Islam, A. Fujisaka, S. Mori, K.R. Ito, T. Yamaguchi, S. Obika, Synthesis and biophysical properties of 5-thio-2, 4-BNA/LNA oligonucleotide, Bioorg. Med. Chem. 26 (12) (2018) 3634–3638.
[28] J. Bentley, J.A. Brazier, J. Fisher, R. Cosstick, Duplex stability of DNA.DNA and DNA.RNA duplexes containing 3′-S-phosphorothiolate linkages, Org. Biomol. Chem. 5 (22) (2007) 3698–3702.
[29] B.E. Lang, F.P. Schwarz, Thermodynamic dependence of DNA/DNA and DNA/RNA hybridization reactions on temperature and ionic strength, Biophys. Chem. 131 (1–3) (2007) 96–104.